

Element Lines: Bonding in the Ternary Gold Polyphosphides, Au_2MP_2 with $M = Pb, Tl, \text{ or } Hg$

Xiao-Dong Wen,[†] Thomas J. Cahill,^{†,‡} and Roald Hoffmann^{*,†}

Department of Chemistry and Chemical Biology, Cornell University, Baker Laboratory, Ithaca, New York 14853-1301; and Department of Chemistry, Hobart and William Smith Colleges, Geneva, New York 14456

Received August 30, 2008; E-mail: rh34@cornell.edu

Abstract: We present a theoretical study of the electronic structures of Au_2PbP_2 , Au_2TlP_2 , and Au_2HgP_2 . Structurally, these compounds contain a framework of condensed Au_2P_6 and Au_4P_6 rings forming parallel channels, which are filled by lead, thallium, or mercury atoms. Given the linear coordination of the Au atoms and the existence of zigzag $-[P-P-P]-$ singly-bonded chains in them, these materials present us with a rare instance of approximately linear, one-dimensional, and zerovalent element (Pb, Tl, or Hg) chains with a variable electron count. The Pb–Pb, Tl–Tl, and Hg–Hg element lines in these structures have somewhat longer bond lengths than their respective single bond lengths or their separations in (calculated) isolated chains. Yet, the zerovalent element interactions are prominent and are responsible for the metallicity of some of these materials. In the calculations, both Au_2PbP_2 and Au_2TlP_2 emerge as metallic, whereas Au_2HgP_2 is a semiconductor. The isolated element chains do not undergo a pairing (Peierls) distortion nor do the chains in the three-dimensional ternaries. The small barrier for mobility of the Pb, Tl, and Hg atoms along the chain axis may explain the large thermal parameters observed in the crystal structures along the chain axis (and the need to use fractional occupations of several positions along the chain). These ternaries may show one-dimensional liquidlike behavior under some conditions.

Introduction

In 2002, the polyphosphide compounds Au_2PbP_2 , Au_2TlP_2 , and Au_2HgP_2 were synthesized and characterized by Eschen and Jeitschko (Figure 1).¹

All three ternary structures feature one-dimensional channels built of Au and P, filled by lead (Pb), thallium (Tl), or mercury (Hg) atoms. The crystal structures of these compounds show two distinct (but as it turns out not very different) Au atoms, Au1 and Au2, one P, and one M atom ($M = Pb, Tl, \text{ or } Hg$). The Au atoms are linearly or nearly linearly coordinated by their neighboring P atoms. The phosphorus atoms form zigzag chains of 2.194 Å; this is close to a typical P–P single bond (~2.22 Å). The phosphorus atoms are approximately tetrahedrally coordinated by two gold and two phosphorus atoms.

Assuming the validity of the octet rule, as well as the electronegativity of the atoms involved, Eschen and Jeitschko suggested (and we certainly concur) that the Au atoms and the P atoms should be assigned oxidation numbers +1 and –1, respectively. Since the ternary compounds are neutral, the Pb, Tl, and Hg atoms must then be in formal oxidation state 0. The Pb–Pb, Tl–Tl, and Hg–Hg distances are 3.236, 3.241, and 3.221 Å in their respective ternary compounds, which are somewhat shorter (except for Hg) than the corresponding elemental distances (Pb: 3.50 Å (fcc);² Tl: 3.41 Å (hcp);³ and

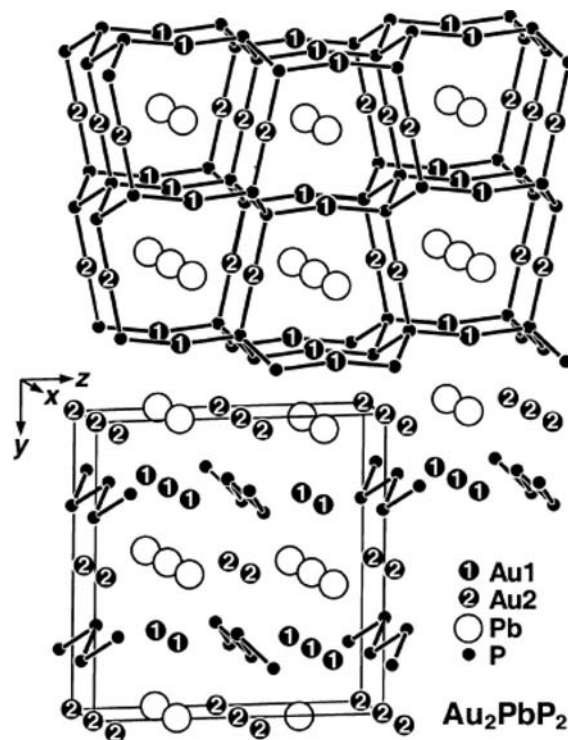


Figure 1. Crystal structure of Au_2PbP_2 ; the illustration is reproduced with permission from ref 1.

Hg: 3.03 Å (rhombohedral)⁴). There is clearly bonding among these linearly aligned element chains. At the same time, the

[†] Cornell University.

[‡] Current address: Hobart and William Smith Colleges.

(1) Eschen, M.; Jeitschko, W. *J. Solid State Chem.* **2002**, *165*, 238.

(2) Mao, H. K.; Wu, Y.; Shu, J. F.; Hu, J. Z.; Hemley, R. J.; Cox, D. E. *Solid State Commun.* **1990**, *74*, 1027.

(3) Barrett, C. S. *Phys. Rev.* **1958**, *110*, 1071.

Table 1. Theoretical Unit Cell Parameters, Bond Lengths (Å), and Angles (deg) of Au_2MP_2 with $M = \text{Pb}, \text{Tl},$ or Hg Calculated with DFT^a

parameter	Au_2PbP_2	Au_2TlP_2	Au_2HgP_2
<i>a</i>	3.20	3.19	3.16
<i>b</i>	11.32	11.31	11.25
<i>c</i>	11.16	11.17	11.16
P–P	2.18	2.18	2.15
P–Au1	2.31	2.32	2.32
P–Au2	2.33	2.32	2.32
M–M	3.20	3.19	3.16
M–Au1	2.86 (3.22)	2.89 (3.20)	2.88 (3.16)
M–Au2	3.23	3.23	3.21
$\angle\text{P–Au1–P}$	166.9	168.3	166.7
$\angle\text{P–Au2–P}$	180.0	180.0	180.0

^a There are two *M*–Au1 bonds in these ternary compounds; the second is indicated in parentheses.

lines are fairly isolated from each other: a typical lateral separation between the two lines is ~ 5.7 Å.

The three ternary gold polyphosphides synthesized by Eschen and Jeitschko thus provide us with materials containing nearly one-dimensional *M*-atom chains, which vary in electron count. One-dimensional materials are pretty rare, and this is a good reason for exploring these compounds theoretically. We begin with a detailed analysis of the lead compound to be followed by its thallium and mercury analogues.

Computational Details. DFT Method. DFT^{5–7} periodic calculations, as implemented in the Vienna ab initio simulation package^{8–14}(VASP) are carried out. For the exchange-correlation functional, the local density approximation (PAW-LDA) is employed with projector augmented wave (PAW) potentials.^{15,16} In all calculations, the energy cutoff for plane waves is 400 eV using a Monkhorst Pack k-point grid.¹⁷

Extended Hückel Theory. After the structures are optimized with DFT, extended Hückel (eH)¹⁸ calculations are performed on each structure, utilizing the YAeHMOP program.¹⁹ The default extended Hückel parameters are employed. The eH calculations are certainly less reliable for structures but offer a number of analytical tools for exploring the nature of bonding. With the DFT program we use, it is difficult to get reliable atomic and orbital contributions to the density of states (DOS).²⁰

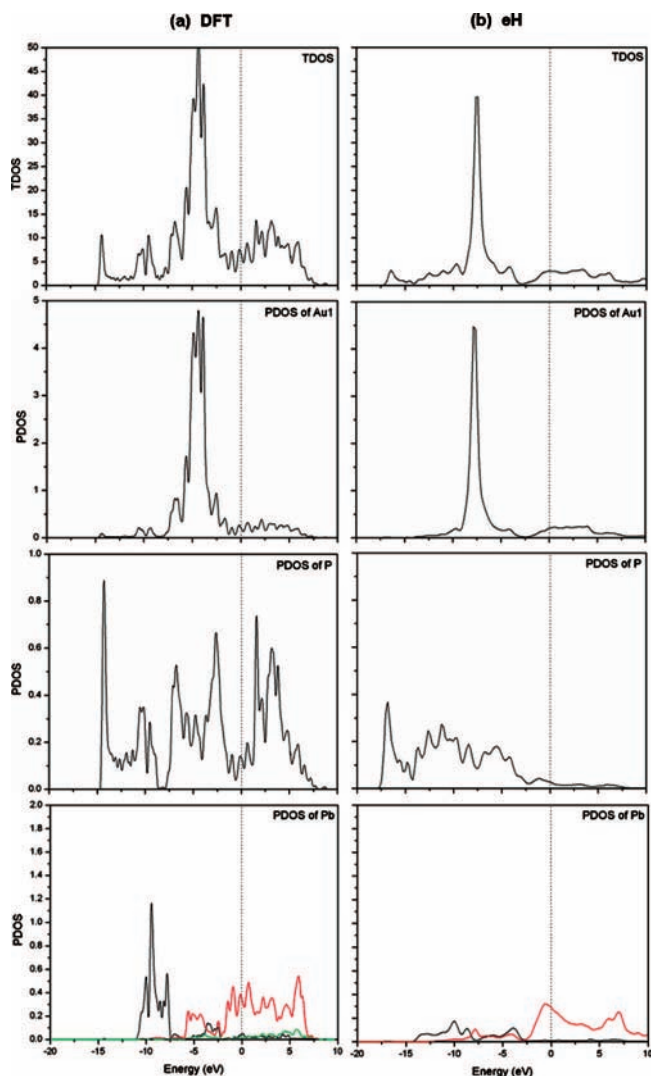


Figure 2. (a) Calculated density of states (DOS) of Au_2PbP_2 (DFT). (b) Calculated DOS of Au_2PbP_2 (eH). The dotted vertical line indicates the adjusted Fermi level at 0 eV. The combined (s + p + d) partial or projected (PDOS) of one P and Au1 atom are shown. The PDOS of Au2 is very similar to the PDOS of Au1. For one Pb atom, the s, p, and d orbital contributions to the DOS are given separately by black, red, and green lines, respectively. Note that the PDOS scales are different for each element.

Crystal and Electronic Structure of Au_2PbP_2 . Utilizing DFT, the unit cell parameters and the bond lengths are computed for Au_2PbP_2 (Table 1) and are found to be within 1.2% of experimentally determined values. For instance, the optimized P–P (2.18 Å) and Pb–Pb (3.20 Å) bond lengths are close to the experimental P–P (2.194 Å) and Pb–Pb (3.236 Å) bond lengths. The space group of this ternary compound, *Cmcm*, forces the P–Au2–P angle to be 180.0°. However, the computed P–Au1–P angle (166.9°) is in good agreement with the experimental data (167.77°). The agreement for the Tl and Hg cases, to be discussed later, is equally good.

Let us look at the electronic structure of Au_2PbP_2 first, and then use the resulting analysis to understand systems containing the Tl and Hg chains. The significant total DOS (TDOS) at the Fermi level (adjusted to 0 eV for easier comparison of eH and DFT results) for Au_2PbP_2 indicates that the compound should be metallic (Figure 2). Eschen and Jeitschko observed metallic luster for all three ternary compounds, but apparently their conductivity was not measured.

- (4) McKeehan, L. W.; Gioffi, P. P. *Phys. Rev.* **1922**, *19*, 444.
- (5) Perdew, J. P.; Chevary, J. A.; Vosko, S. H.; Jackson, K. A.; Pederson, M. R.; Singh, D. J.; Fiolhais, C. *Phys. Rev. B* **1992**, *46*, 6671.
- (6) Perdew, J. P.; Chevary, J. A.; Vosko, S. H.; Jackson, K. A.; Pederson, M. R.; Singh, D. J.; Fiolhais, C. *Phys. Rev. B* **1993**, *48*, 4978.
- (7) Perdew, J. P.; Burke, K.; Ernzerhof, M. *Phys. Rev. Lett.* **1996**, *77*, 3865.
- (8) Perdew, J. P.; Burke, K.; Ernzerhof, M. *Phys. Rev. Lett.* **1997**, *78*, 1396.
- (9) Kresse, G.; Hafner, J. *Phys. Rev. B* **1993**, *47*, 558.
- (10) Kresse, G.; Hafner, J. *Phys. Rev. B* **1994**, *49*, 14251.
- (11) Kresse, G.; Hafner, J. *J. Phys.: Condens. Matter* **1994**, *6*, 8245.
- (12) Kresse, G.; Furthmüller, J. *Comput. Mater. Sci.* **1996**, *6*, 15.
- (13) Kresse, G.; Furthmüller, J. *Phys. Rev. B* **1996**, *54*, 11169.
- (14) Kresse, G.; Joubert, D. *Phys. Rev. B* **1999**, *59*, 1758.
- (15) Blochl, P. E. *Phys. Rev. B* **1994**, *50*, 17953.
- (16) Kresse, G.; Joubert, D. *Phys. Rev. B* **1999**, *59*, 1758.
- (17) Monkhorst, H. J.; Pack, J. D. *Phys. Rev. B* **1976**, *13*, 5188–5192.
- (18) Hoffmann, R. *J. Chem. Phys.* **1963**, *39*, 1397.
- (19) Landrum, G. A. Viewkel, Version 3.0. Viewkel is distributed as part of the YAeHMOP extended Hückel molecular orbital package and is freely available on the Internet at <http://overlap.chem.cornell.edu:8080/YAeHMOP.html>.
- (20) The RWIGS values for Pb (1.725 Å), P (1.233 Å), and Au (1.503 Å) are the default parameters from the pseudopotential file. There are real problems with VASP projected DOS values not adding up to the total DOS.

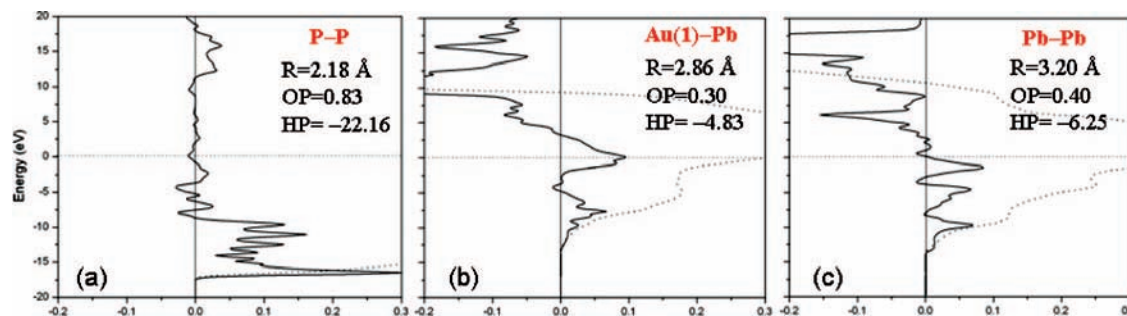


Figure 3. Crystal orbital overlap population (COOP, eH method) curves for bonds in Au_2PbP_2 . The corresponding distances as well as the OP and HP values are listed (integrated up to the Fermi level). The solid line represents the COOP curve, while the dotted line represents the integration. The dotted horizontal line indicates the adjusted Fermi level at 0 eV.

The contributions to the DOS are explored utilizing partial densities of states (PDOS), with DFT (Figure 2 and Figure S1 in the Supporting Information). For Au, the d orbitals are almost completely filled (DOS between -2.5 and -8 eV), as one would expect from its $[\text{Xe}]5d^{10}$ configuration (for Au^{1+}). The 6p and 5d orbitals of the Au atoms contribute little at the Fermi level. The 3p orbital of P is partially filled (there is substantial s and p density above the window of the graph). The Fermi level falls in a region with no P density; the 3s orbital of P is found far below. For Pb, it is clear that the crystal orbitals derived from the 6s are also found far below the Fermi level. There is not much s-p mixing for Pb. However, the 6p orbital of Pb is partially filled and crosses the Fermi level. This indicates that the Pb atoms play an important role in the metallic behavior of Au_2PbP_2 .

The contributions to the DOS are also explored with the eH method (Figure 2b). In general, the DOS and its decompositions are similar in the two methods. The apparent discrepancy on the P states (few states above the Fermi level) is not serious: the eH calculations have a good number of unoccupied p orbital states above the energy window selected. However, eH calculations indicate substantial mixing between the 3s and 3p orbitals of P and between the 6s and 6p orbitals of Pb. In contrast to DFT, eH calculations show a significant contribution from the Au 6p orbital at the Fermi level. Clearly, there is more s-p mixing indicated in eH than in DFT calculations. Since there are real problems with the PDOS calculations in the DFT procedure employed, we do not know which method to trust in this matter; we will continue employing both, taking advantage of the strengths of each. To be specific, we will use DFT for energetics and eH for analysis of bonding.

Where are the Bonds? The density of states only gives information about the location of electrons but not about the character of the bonds. In order to analyze the bonding in Au_2PbP_2 , we employed both crystal orbital overlap populations (COOP) and crystal orbital Hamilton populations (COHP; Figure 3 for selected bonds; all bonds and respective COOP curves shown in Figure S2 in the Supporting Information). The strength of the bonds can be gauged with COOP calculations; positive and negative regions are bonding and antibonding, respectively, as measured by a Mulliken overlap population.²¹ COHP is an energy partitioning, with negative values indicating bonding.

(a) P–P. The P–P OP is 0.83, as shown in Figure 3a, but is that typical of a single bond? We computed the OP of different PP bonds in simple compounds, as a comparison standard: (1)

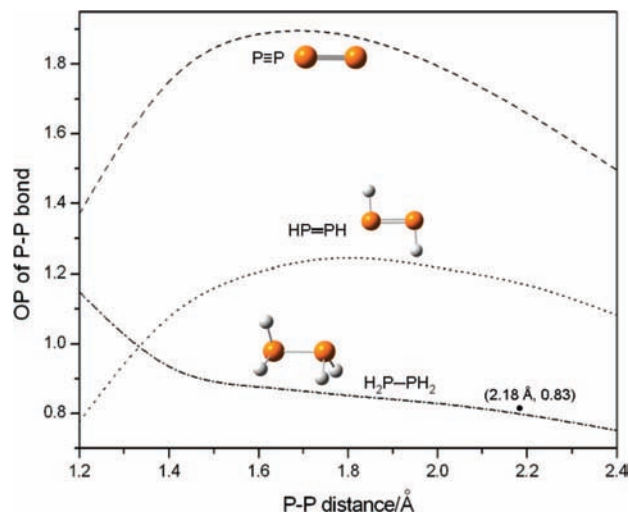


Figure 4. OP for different PP bonds in molecular models for a P–P single bond ($\text{H}_2\text{P}-\text{PH}_2$), a double bond ($\text{HP}=\text{PH}$), and a triple bond ($\text{P}\equiv\text{P}$). The solid dot (distance and OP displayed) in the lower right corner marks the location of the P–P bond in Au_2PbP_2 .

a single bond in $\text{H}_2\text{P}-\text{PH}_2$; (2) a double bond in $\text{HP}=\text{PH}$; (3) a triple bond in $\text{P}\equiv\text{P}$ (Figure 4). The OP of the P–P chain in Au_2PbP_2 indicates a single bond. The P–P single bond distance in many known compounds is around 2.19 Å to 2.26 Å.^{22,23}

(b) Au–Pb. Three different Au–Pb distances are observed in this ternary compound: two different Au1–Pb contacts (2.86 Å and 3.22 Å) and one Au2–Pb (3.23 Å). For the shortest bond among these, the HP value (-4.83 eV) is substantial (Figure 3b). Furthermore, the Fermi level falls into a region of Au–Pb bonding. This result is interesting, as it indicates that a simplistic model of Pb, Tl, or Hg lines sitting in an “inert” channel is only a first approximation. There are clearly some covalent interactions between the channel atoms (especially Au1) and Pb, as demonstrated by the HP value cited and the 2.86 Å Au1–Pb distance, which is similar to the sum of the atomic radii of Au (1.34 Å) and Pb (1.54 Å). The interaction of the Pb atoms with the other Au ions lining the channel is much weaker than the one shown in Figure 3b.

We probed the Au1–Pb interaction further by computing a $[\text{PH}_3-\text{Au}-\text{PH}_3]^{1+}$ system (details not given here). This molecular model has a pair of nearly pure Au 6p LUMOs. It is primarily these orbitals that interact with the Pb atoms.

(21) Hoffmann, R. *Solids and Surfaces: A Chemist's View of Bonding in Extended Structures*; Wiley-VCH: New York, 1988.

(22) Hoffmann, R.; Zheng, C. *J. Phys. Chem.* **1985**, *89*, 4175.

(23) Emsley, J.; Hall, D. *The Chemistry of Phosphorus*; Harper and Row: London, 1976.

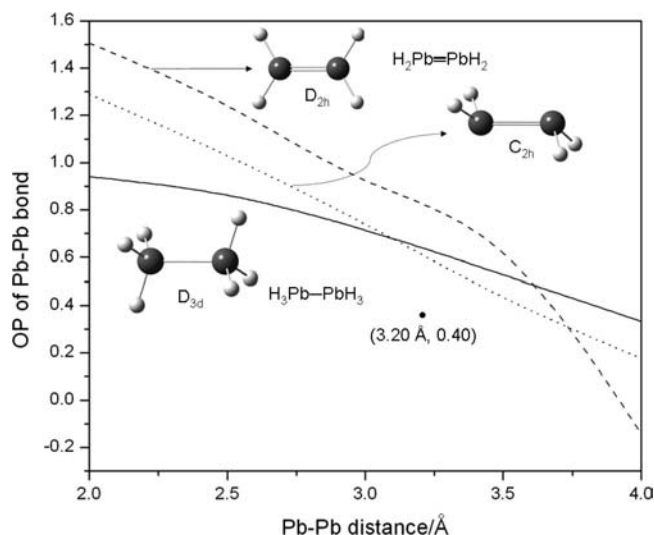


Figure 5. How the OP varies with PbPb distance for various molecular compounds containing PbPb bonds: a Pb–Pb single bond ($\text{H}_3\text{Pb–PbH}_3$, D_{3d} , solid line), a double bond ($\text{H}_2\text{Pb=PbH}_2$, D_{2h} and C_{2h}). The solid dot marks the distance and OP of the Pb–Pb chain in Au_2PbP_2 .

(c) **Pb–Pb.** The unique characteristic of Au_2PbP_2 is the element line consisting of Pb atoms. The Pb–Pb bond length is 3.20 Å, perforce the same value as the unit cell parameter a . The Pb–Pb distance in Au_2PbP_2 is a little longer than the sum of atomic radii of two Pb atoms (3.08 Å). For the Pb–Pb interaction shown in Figure 3c, both the OP (0.40) and the HP (–6.25 eV) indicate Pb–Pb bonding. But, how much?

For calibration, the OP as a function of distance was computed for a prototypical Pb–Pb single bond (H_3PbPbH_3) and a hypothetical double bond (H_2PbPbH_2) with two different geometries (Figure 5).²⁴ It is apparent that the Pb–Pb OP in Au_2PbP_2 falls below the single (or double; we do not want to enter here the important but vexing discussion on multiple Pb–Pb bonding) bond zone but not by much; the Pb–Pb bonding in the channels is substantial, even if it is relatively weak.

Turning to experiment, Power's²⁵ review of group 14 dimers shows *trans*-bent alkene congeners with Pb–Pb distances of 2.990 Å in $[\text{Pb}\{\text{Si}(\text{SiMe}_3)_3\}\text{Trip}]_2$ and 3.052 Å in $\text{Trip}_2\text{PbPbTrip}_2$. Interestingly, these distances are longer than the single bond lengths found in similar R_3PbPbR_3 compounds ($\text{Ph}_3\text{PbPbPh}_3$, Pb–Pb = 2.85 Å).²⁶ In the extended $\text{Ti}_6\text{Pb}_{4.8}$ structure, Kleinke²⁷ observed one-dimensional, nonisolated Pb chains (Pb–Pb = 2.895 Å). In this extended structure, the Pb–Pb bond is noticeably shorter than the typical Pb–Pb single bond (3.10 Å).

In Au_2PbP_2 , two similar Au–P bonds are observed: Au1–P (2.31 Å) and Au2–P (2.33 Å), both of which are within the range of experimental and theoretical Au(I) phosphine complex distances (2.270–2.460 Å).^{28–32} In addition, the large calculated negative HP values (–15.46 eV for Au1–P, –15.31 eV for Au2–P) support strong Au–P bonding.

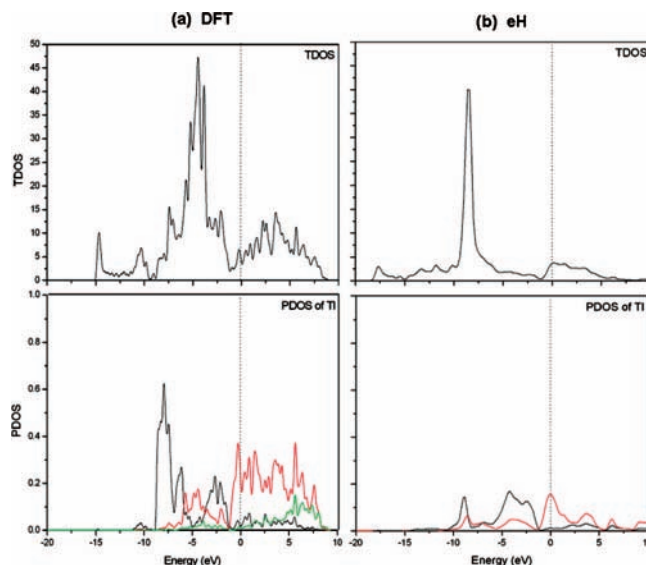


Figure 6. (a) Calculated DOS of Au_2TIP_2 (DFT). (b) Calculated DOS of Au_2TIP_2 (eH). The dotted vertical line indicates the adjusted Fermi level at 0 eV. The s, p, and d orbital contributions to the TI DOS are represented by black, red, and green lines, respectively. The PDOS of one TI atom is shown. Note that the DOS scales are different.

There is no Au–Au bonding to speak of, as indicated by the small OP value of 0.01. In molecular systems, at similar separations (~ 3.20 Å) between Au atoms, one sometimes observes weak bonding termed *aurophilic*.^{33,34}

Au_2TIP_2 and Au_2HgP_2 . Au_2TIP_2 and Au_2HgP_2 are isotopic with Au_2PbP_2 . The DFT optimized structural parameters are shown in Table 1. They are within 2% of the observed structures. We will return later to the fractional occupancy of several sites that was needed in the Eschen and Jeitschko refinement.

Let us look at the electronic properties of Au_2TIP_2 and Au_2HgP_2 . The Au and P PDOS in both compounds (not shown here, but in Figures S3 and S4 in the Supporting Information) are similar to those seen in Figure 2 for Au_2PbP_2 . The total DOS at the Fermi level for Au_2TIP_2 indicates that the compound should be metallic (Figure 6). The PDOS shows the TI p orbitals cross the Fermi level; thus, the TI chain is responsible for the metallicity of Au_2TIP_2 .

Should we expect the same behavior for Au_2HgP_2 ? No, our analysis of isoelectronic Pb^{2+} indicates a large gap at the Fermi level. For Hg, $[\text{Xe}]5d^{10}6s^2$, the 6s and 5d bands are filled, and there is a real gap to the 6p band. To no surprise, the TDOS of Au_2HgP_2 has a pseudogap at the Fermi level (Figure 7), and the PDOS of Hg shows no significant contributions at this energy. The calculated band structure (Figure S9 in the Supporting Information) confirms the existence of a real (albeit small) energy gap at the Fermi level.

Au_2P_2 Framework, without the Element Lines. To explore the role of the M atoms in the ternary compound, the M – M element lines were removed. The optimized lattice constants a , b , and c for the resulting hypothetical Au_2P_2 complex are 3.17,

(24) Pb=Pb bonds are *trans*-bent pyramidalized; the computations here are for both a planar and *trans*-bent pyramidalized geometry.

(25) Power, P. P. *Chem. Rev.* **1999**, *99*, 3463.

(26) Kleiner, N.; Dräger, M. *Acta Crystallogr. Sect. B* **1979**, *35*, 573.

(27) Kleinke, H. *J. Solid State Chem.* **2001**, *159*, 134.

(28) Schwerdtfeger, P.; Hermann, H. L.; Schmidbaur, H. *Inorg. Chem.* **2003**, *42*, 1334.

(29) Schwerdtfeger, P.; Boyd, P. D. W.; Burrell, A. K.; Robinson, W. T. *Inorg. Chem.* **1990**, *29*, 3593.

(30) Shapiro, N. D.; Toste, F. D. *Proc. Natl. Acad. Sci. U.S.A.* **2008**, *105*, 2779.

(31) Zank, J.; Schier, A.; Schmidbaur, H. *Z. J. Chem. Soc., Dalton Trans.* **1999**, *3*, 415.

(32) Jeitschko, W.; Möller, M. H. *Acta Crystallogr. Sect. B* **1979**, *35*, 573.

(33) Pyykkö, P.; Runeberg, N.; Mendizabal, F. *Chem. Eur. J.* **1997**, *3*, 1451.

(34) Schmidbaur, H.; Schier, A. *Sci. Synth.* **2004**, *3*, 691.

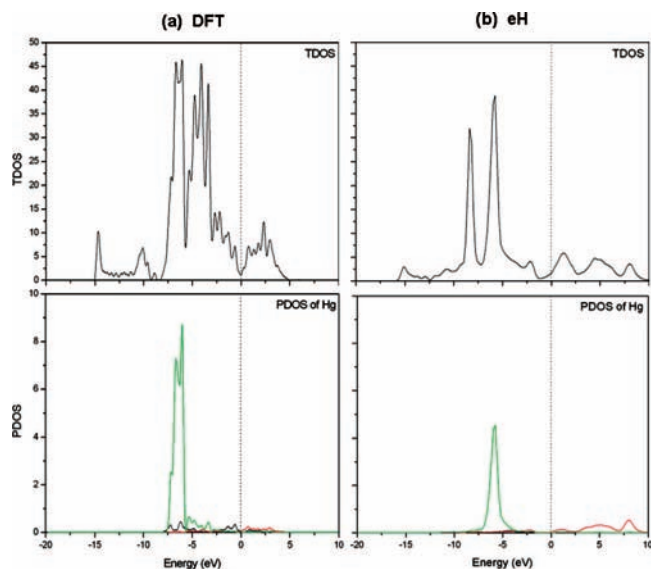


Figure 7. (a) Calculated DOS of Au_2HgP_2 (DFT). (b) Calculated DOS of Au_2HgP_2 (eH). The dotted vertical line indicates the adjusted Fermi level at 0 eV. The Hg s, p, and d orbital contributions to the DOS are represented by black, red, and green lines, respectively. The PDOS of one Hg atom is shown. Note that the DOS scales are different.

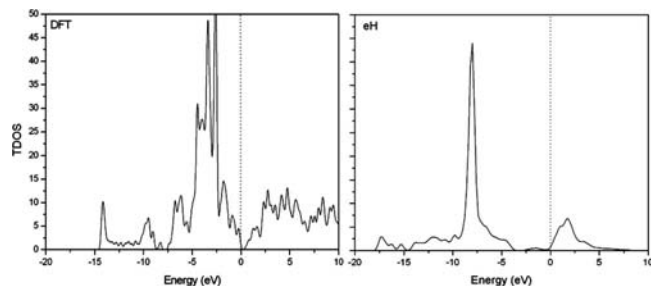


Figure 8. TDOS calculated for Au_2P_2 with DFT and eH. The dotted vertical line indicates the adjusted Fermi level at 0 eV.

11.08, and 11.18 Å, respectively. In comparison with Au_2PbP_2 , the Au_2P_2 lattice vectors, **a** and **b**, are smaller by 2.0% and **c** by 0.2%. It appears that the framework is “stable” without the element lines; including the lines (along **a**) leads to expansion of the lattice and is, as we saw from the OP values, stabilizing.

Might Au_2P_2 be a real compound? The actual Au–P phase diagram is surprising: there exists only one binary compound of these two elements, Au_2P_3 .³⁰ For Au_2P_2 , aside from the possibility derived from the ternaries, other structures are certainly imaginable (e.g., the PtS structure and other networks consistent with square-planar Au^{3+} and tetrahedral P^{3-}). We will return later to a hypothetical Au_2MP_2 with $M = \text{Au}$ (“ Au_3P_2 ”), but a full theoretical investigation of the Au–P phase diagram remains for the future.

As Figure 8 shows, Au_2P_2 (an electron precise compound, with Au^{1+} and $(\text{P}^{1-})_n$ chains) is a semiconductor, with a small gap (larger with eH) at the Fermi level. Clearly, the presence of the M – M chains in the channels of the Au_2P_2 lattice is responsible for the metallicity of Au_2MP_2 with $M = \text{Pb}$ or Tl.

Scrutinizing the Element Lines: A One-Dimensional Model for the Pb Chain. In order to better understand the electronic structure of the element lines in the Au_2PbP_2 compound, a simple one-dimensional chain of Pb atoms (one atom per unit cell) with a length of 3.20 Å was computed and analyzed with the eH method (Figure 9). The band structure is

Table 2. Calculated Pb–Pb OP and Fermi Level (eV) of Au_2PbP_2 and of the Hypothetical Sublattices ($[\text{PbP}_2]_4^{8-}$, $[\text{Pb}]_\infty^{0.70}$, and $[\text{Pb}]_\infty^0$)^a

	Pb–Pb OP	Fermi level (eV)
Au_2PbP_2	0.40	−7.35
$[\text{PbP}_2]_4^{8-}$	0.30	−5.20
$[\text{Pb}]_\infty^{0.70}$	0.54	−8.77
$[\text{Pb}]_\infty^0$	0.59	−8.29

^a The parameters and positions of the remaining atoms were not changed from those computed in Au_2PbP_2 .

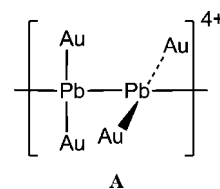
just about what would be expected for a moderately interacting one-dimensional array of main group atoms.²¹ The bands built up by Pb 6s and 6p_z (*z* is the line axis) orbitals have positive and negative slopes. The COOPs show weak, but noticeable s–p_z mixing. The Fermi level (for a neutral chain) passes through the p_z and π (p_x, p_y) bands.

The isolated Pb–Pb chain was optimized with DFT, yielding a Pb–Pb bond distance of 2.80 Å. Note that this distance is somewhat shorter than the spacing enforced by the gold polyphosphide lattice (3.20 Å). There is some stress in the Au_2PbP_2 structures.

The Pb–Pb OP and HP for the isolated one-dimensional chain is 0.59 and −9.69 eV, respectively, larger in magnitude than for the corresponding element lines (0.40 and −6.25 eV) existing in the channels. The Fermi level in the isolated chain is lower, and the Pb–Pb bond is stronger than in the ternary. There are several possible reasons for this, which we explored:

(1) The interaction of the Pb line with the Au_2P_2 network changes the electron count in the chain. The eH charge on each Pb in Au_2PbP_2 is +0.70. The OP in the corresponding polymer is 0.54 (Table 2), but the Fermi level is naturally lower.

(2) Pb–Au interactions spread the levels of the Pb line and change its bonding. We probed this in two ways: by (a) removing the 8Au¹⁺ from the $Z = 4$ $[\text{Au}_2\text{PbP}_2]_4$ ternary (i.e. calculating $[\text{PbP}_2]_4^{8-}$) and (b) adding two external Au¹⁺ to each Pb in a one-dimensional Pb chain, $[(\text{PbAu}_2)_2]_\infty^{4+}$, as shown in **A**. The first option gives a Pb–Pb OP of 0.30, even lower than the ternary Pb–Pb OP. The second approach (several structural variants on **A** were also attempted) gives a Pb–Pb OP also around 0.30 (Table 2).



We conclude that both effects, interaction with Au^{1+} and charging of the Pb chain, contribute, difficult as they are to take apart.

Tl and Hg Lines. An important aspect of these structures is the electronic tuning provided by the replacement of Pb with Tl or Hg. There is a change due to the inherent difference in the elements, and there is a change due to the level filling: Tl has one less electron, Hg two less. In a frozen band approximation (using the Pb bands to reason about the Tl and Hg structures), the M – M bonding should weaken as one removes electrons, and the Hg line may show a band gap, as the s and d bands should be filled.

Let’s see what happens with “real” Tl and Hg chains. The Tl chains are similar to the Pb chains in their behavior. For example, both the computed Pb and the Tl have π contributions

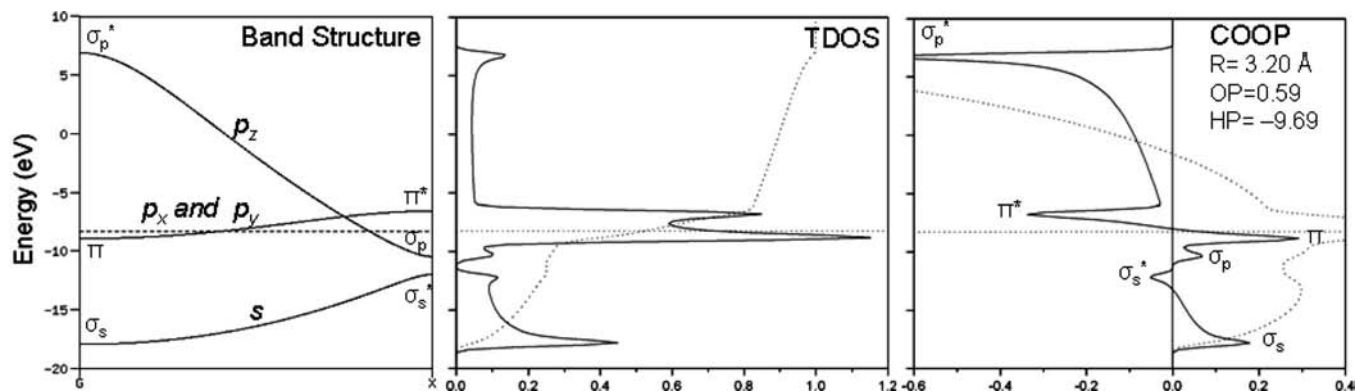


Figure 9. Band structure, TDOS and COOP of a one-dimensional Pb–Pb chain (Pb–Pb = 3.20 Å) calculated with the eH method. The dotted horizontal line indicates the Fermi level.

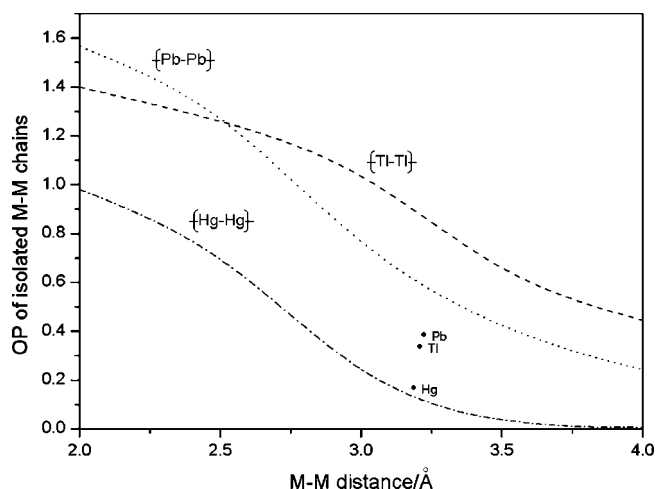


Figure 10. Overlap population of isolated *M* chains (Pb, Tl, or Hg) as a function of varying bond lengths (eH): The dot marks the location of the OP for the Pb, Tl, and Hg chains in their ternary compounds.

at the Fermi level. On the other hand, the computed Hg chains have a large gap at the Fermi level. (further details in Section SB of the Supporting Information). The OPs for the one-dimensional isolated Pb, Tl, and Hg chains are computed as a function of bond distance (Figure 10). Interestingly, a decrease in *M*–*M* bonding is predicted for both the Pb chains and the Tl chains upon entering into the Au_2P_2 channel, while for Hg there is a small increase in bonding. The effect is largest for Tl.³⁵

Possible Peierls Distortion of the *M*–*M* Linear Chains. One-dimensional chains with partially filled bands are prone to undergo Peierls distortions, alternatively viewed as electron–phonon coupling. In general, these lower the energy of the system and create a gap at the Fermi level. Dimerization, leading to alternating long and short bonds, is the common consequence for a half-filled band. We begin by probing the potential Peierls distortions in the element lines by investigating three one-dimensional Pb chains: (a) a linear chain (**1**) and (b) two planar zigzag chains (**2** and **3**). The geometries are shown in Table 3.

For the linear Pb chain, all simple pairing distortions led back to the linear polymer geometry. The absence of a Peierls distortion was at first sight surprising. When a one-dimensional congeneric C chain is modeled, the expected Peierls distortion

Table 3. Structures, Geometrical Parameters, and Energies of Isolated Pb Chains (DFT) are Shown^a

Structure	Distances and Angles	E_f (eV/per atom)
	1 a=b=2.80 Å	–2.25
	2 a=b=2.82 Å, $\alpha=114^\circ$	–2.47
	3 a=b=3.10 Å, $\alpha=60^\circ$	–2.92

^a The formation energy (E_f) per Pb atom in the unit cell is calculated: $E_f = 1/2[(\text{energy of Pb chain for 2 atoms in unit cell}) - (2 \times \text{energy of Pb atom})]$.

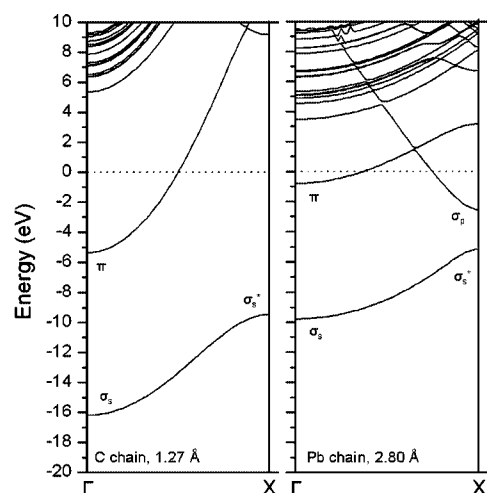
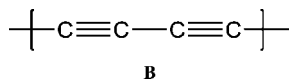


Figure 11. Band structures (DFT) of the optimized C linear chain (1.27 Å) and the Pb linear chain (2.80 Å) with one atom per unit cell. The main orbital contributions are shown.

is observed, with a band gap opening for a half-occupied π band (See Figure 11, left, before pairing distortion). The distorted carbon structure (carbyne) that emerges has been much discussed in the literature.³⁶ The ensuing bond alternation in such a carbyne chain is consistent with a polyacetylenic valence structure, **B**.

Clearly, a Pb chain is different (note in the right-hand panel of Figure 11 that the σ_p band now penetrates the π band and comes below it). There is less s–p mixing for Pb than for C.

(35) Note the difference in these curves for the Pb single and double bond models of the structures, inset in Figure 5; the isolated line for Pb features some multiple bonding.



The Fermi level does not half-fill either the π or the σ_p band, so the simplest Peierls distortion does not occur.

However, we found more complicated stabilizing distortions with $Z = 2$, two atoms per unit cell. Two different zigzag structures, **2** and **3**, were obtained when the optimization is performed from a nonlinear starting geometry. The Pb atoms in **2** are coordinated by two Pb atoms with a Pb–Pb distance of 2.82 Å and a Pb–Pb–Pb angle of 114°. However, the Pb atoms in **3** are coordinated by four Pb atoms with a Pb–Pb distance of 3.10 Å and a Pb–Pb–Pb angle of 60°. Both structures are metallic.

An interesting question is whether there exists a barrier to this increase in dimensionality. We have probed this by building a potential energy surface relating **1**, **2**, and **3** (Figure 12). There is essentially no barrier (<0.01 eV) between linear chain **1** and ribbon **2** and only a small barrier (~0.06 eV) between the two ribbon geometries. Such barriers, conferring metastability and possible kinetic persistence on lower dimensional materials, are likely to be highest for C.

Though we do not find a Peierls distortion for an isolated Pb chain, could the tension occasioned by fitting that chain into the Au_2P_2 “box” (with its stretched repeat distance of 3.20 Å) activate the pairing distortion? Calculations utilizing a $2 \times 1 \times 1$ super cell of Au_2PbP_2 indicate no tendency toward distortion in the Pb chains. We have not explored deviations from stoichiometry that might accommodate such distortions (e.g., y Au per x Pb, where $y/x \neq 2$).

Returning to simple, isolated Pb chains, there are other, still more stable structures than **2** or **3**. The Pb chain may coil up in a helix, make a ladder, and build more complicated structures. It turns out that all of the other computed structures (see Figure S14 in the Supporting Information) are preferred over the linear chain.

Is this a surprise? It should not be, as such ribbons, helices, and ladders are essentially ways of increasing dimensionality; they are stages in moving from a one-dimensional to a two-dimensional and eventually to a three-dimensional structure. In the case at hand, elemental Pb, in the face centered cubic (fcc) lattice, is the expected limit of these distortions.³⁷ Its computed (DFT) formation energy is -3.83 eV on the scale shown. To put it another way, the Pb atoms desire more neighbors than a linear geometry provides. They can get them within a one-dimensional constraint by bending, kinking, and/or curling up in a variety of ways.

Pb dimer chains have been observed experimentally on a Si(100) surface with STM.³⁸ Theoretical work also describes Pb dimer chains on Si(100).³⁹ Chan et al. suggested that these Pb dimer chains form near step edges of the Si(100) substrate.⁴⁰

(36) Fehlner, T. P.; Halet, J.-F.; Saillard, J.-Y. *Molecular Clusters*; Cambridge University Press: Cambridge, U.K., 2007.

(37) We have found instances in elemental structures where variants of a structure are nearly equal (or possibly lower) in energy to the observed bulk structures (work to be reported elsewhere): not that they will be easy to make.

(38) Dong, Z. C.; Fujita, D.; Nejoh, H. *Phys. Rev. B* **2001**, *63*, 115402.

(39) Gonzalez-Mendez, M. E.; Takeuchi, N. *Phys. Rev. B* **1998**, *58*, 16172.

(40) Chan, T.-L.; Wang, Z. C.; Lu, Z.-Y.; Ho, K. M. *Phys. Rev. B* **2005**, *72*, 045405.

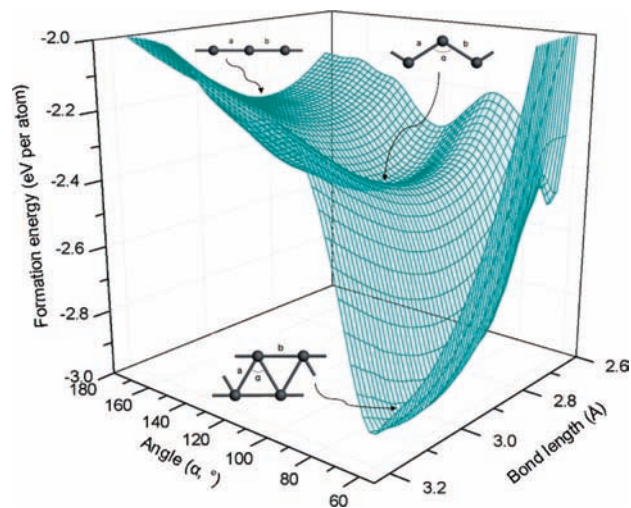


Figure 12. The potential energy surface relating **1**, **2**, and **3**, computed from single point DFT calculations. The formation energies per atom in a unit cell, bond lengths, and angles are shown.

Table 4. Relative Total Energy per Unit Cell (eV) for the Three Ternary Compounds as the Metal Atom Chains (Four M Chains/Unit Cell) are Slid through the Channel^a

	initial (P_0)	step 1	step 2	step 3	step 4 (P_f)
Au_2PbP_2	[0]	0.11	0.43	0.84	1.07
Au_2TlP_2	[0]	0.10	0.40	0.79	1.08
Au_2HgP_2	[0]	0.09	0.32	0.62	0.74

^a The energies are referred relative to that for P_0 .

Recently, coupled Pb chains were found experimentally by Tegenkamp et al. on a Si(557) surface.⁴¹

Recently, Höhn et al.⁴² reported a study of the ternary nitrides $\text{Ga}_7\text{N}_4\text{M}_x$, which contain one-dimensional chains similar to the Au_2MP_2 compounds ($M = \text{Pb}, \text{Tl}, \text{or Hg}$). These linear chains are referred to as “guests in a subnitride host.” Höhn et al. suggested that the interaction between the M chain and the channel inhibits a Peierls distortion.

Sliding the Chains through the Lattice. Could the metal atoms occupy different positions along the chain in these ternary compounds, and if so, might this cause the metal chains to buckle slightly? A small potential energy surface was probed to locate other energy minima (Table 4). The M chain atoms were gradually moved a total distance of 1.6 Å in the \mathbf{a} direction (along the channel, in four 0.4 Å steps from P_0 to P_f) in single point calculations without changing the optimized M – M distances in Au_2MP_2 (displayed in Scheme 1). Note that there are four M atoms (thus, four M chains) per unit cell; all chains were shifted in the same direction and by the same amount.⁴³ As the metal chain atoms (Pb, Tl, or Hg) were shifted further from their optimized positions, the total energy increased.

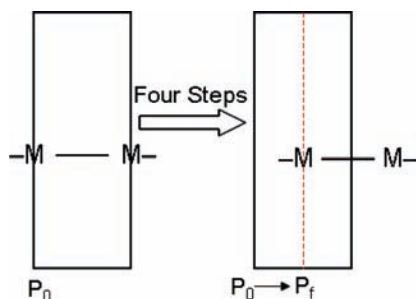
To put it another way, we have calculated here an approximate barrier to the Pb chains sliding along the channel axis of 1.07 eV per 4 Pb atoms (~6 kcal/Pb atom). This energy is small, comparable with the typical activation barriers observed for ionic conduction (~11 kcal, under elevated pressure and

(41) Tegenkamp, C.; Ohta, T.; McChesney, J. L.; Dil, H.; Rotenberg, E.; Pfnür, H.; Horn, K. *Phys. Rev. B* **2008**, *100*, 076802.

(42) Höhn, P.; Auffermann, G.; Ramlau, R.; Rosner, H.; Schnelle, W.; Kniep, R. *Angew. Chem., Int. Ed.* **2006**, *45*, 6681.

(43) The geometries of the channel are not changed, and the M – M distance is held constant (Pb–Pb = 3.20 Å; Tl–Tl = 3.19 Å; Hg–Hg = 3.16 Å).

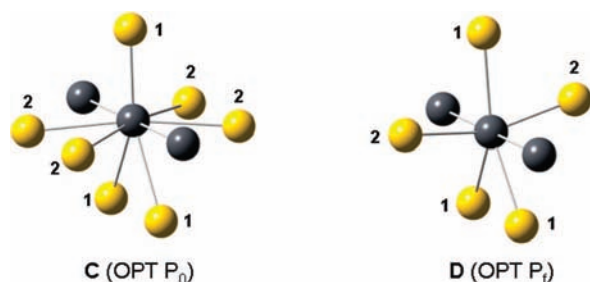
Scheme 1. Simplified Picture of the Relative Initial (P_0) and Final Position (P_f) of the Metal Chain, as It Slides through the Channel



temperature).^{44,45} The possibility of chain mobility (or liquidlike behavior at slightly elevated temperatures) is fascinating. The small barrier for Pb motion along the chain axis (and the still smaller barrier for Hg) may also explain the large thermal parameters along the chain axis observed in the crystal structures and the refinement that required alternative sites for Hg (and Tl).

Next, optimizations were performed to determine if any of these single point geometries (Steps 1, 2, 3, or 4 as shown in Table 4) might “activate” buckling of the chain. The symmetry was not constrained in these optimizations. Depending on the initial point of the chain in the channel, two different energy minima were found for each ternary compound. Optimizations beginning in Step 1 or 2 geometries, all (for all three ternary compounds) reverted back to their initial P_0 structures, labeled OPT P_0 . But, optimizations starting from the Step 3 or 4 geometries converged to new structures, with the same $Cmcm$ group, labeled OPT P_f (as the M chains most closely resembled the geometries utilized in Step 4 of the single point calculations).

In what way are the OPT P_f structures different from the OPT P_0 ones? Overall, the answer is “not much.” The differences in unit cell parameters and distances are less than 2%. However, there is an essential and obvious change in Pb (and Au2) coordination as indicated in Structures **C** and **D** with Pb = black, Au1 = 1, and Au2 = 2. Note that the four 4-fold coordination of Pb by Au2 in OPT P_0 is now 2-fold in OPT P_f .



If the barrier to sliding the lines through the lattice is taken as $[E(\text{OPT } P_f) - E(\text{OPT } P_0)]$, we are led to an activation barrier per four chains in a unit cell of 0.25 eV (Pb), 0.12 eV (Tl), and -0.06 eV (Hg). Per chain, this energy comes to less than 0.07 eV = 1.6 kcal/atom of M . That is a really small energy, which helps us understand the large anisotropic displacement parameters and the need for alternative sites in the structural refinement.

Table 5. Optimized Bond Lengths (\AA , with DFT) of Different $M-M$ Chains Placed in Au_2MP_2

structure	$M-M$ distance (\AA)	structure	$M-M$ distance (\AA)
Au_2PbP_2	3.20	Au_2SnP_2	3.16
Au_2TlP_2	3.19	Au_2CdP_2	3.14
Au_2HgP_2	3.16	Au_2IP_2	3.25
Au_2BiP_2	3.21	Au_2ZnP_2	3.12
Au_2InP_2	3.14	Au_2TeP_2	3.18
Au_2SbP_2	3.16	Au_2AuP_2	3.05

There are some interesting differences among the three polyphosphides, to which we alluded. The structural refinement by Eschen and Jeitschko for the Tl and Hg cases indicates fractional occupation of several M positions along a line. There is also a large U_{ii} (anisotropic displacement parameters) for the atoms in the channel. The position of the Hg atoms is the least well determined followed by Tl and then Pb. The indication in the mercury and thallium compounds is of disorder or atom mobility along the chain. Other than the clear finding that such mobility is theoretically easy, we have not investigated theoretically (it would be difficult to do so) the potential of fractional site occupation.

We suggest that one look experimentally for the indicated high mobility of these element chains.

Threading Other Chains through Au_2P_2 . To the best of our knowledge, only Au_2MP_2 with $M = \text{Pb, Tl, or Hg}$ have been prepared. In the hope that other ternary gold polyphosphides will be investigated, we modeled a series of Au_2MP_2 compounds with $M = \text{Zn, Cd, In, Sn, Sb, Te, I, Bi, or Au}$ (Table 5; unit cell parameters shown in Table S8 of the Supporting Information). Some of these are congeners of the known ternary compounds, others are quite hypothetical. We did not study structural alternatives for any of these compounds. Once the geometries of the compounds were optimized (DFT), eH computations were carried out. The OP and HP of these hypothetical element lines are smaller than those of the corresponding isolated one-dimensional chains (except in Hg and Cd). HP analysis, unlike OP, can be utilized to compare the bonding properties of different atoms. There is clear indication of bonding in the chains for all these hypothetical phases (Sb–Sb chains have been studied extensively in the literature).⁴⁶

Iodine is especially interesting, as infinite I–I chains only exist in organic complexes. The 3.25 \AA I–I distance computed for Au_2IP_2 is significantly shorter than the van der Waals I...I interaction (4.30 \AA) and longer than the molecular I_2 bond length (2.67 \AA). Is the predicted I–I distance in Au_2IP_2 realistic? It would seem so, based on the only well-studied infinite polyiodide chain, in the starch-iodine complex.⁴⁷ The starch-iodine complex has an average I–I separation of 3.1 \AA , similar to the 3.25 \AA I–I distance in Au_2IP_2 . Although the I–I OP in Au_2IP_2 (0.15) seems small, the molecular I_2 OP is only 0.49 at the much shorter separation of 2.67 \AA .

As mentioned earlier, only one binary Au–P compound is known to date, Au_2P_3 . One obvious idea for generating an alternative is to fill the Au_2P_2 channel structure with a Au line (i.e., Au_3P_2 , listed in Table 5). This structure turns out to be metallic. We also computed the known Au_2P_3 structure and found it to have a large pseudogap. The ΔE computed (8Au(fcc)

(44) Hassan, M. *Res. Lett. Phys.* **2008**, *2008*, 1.

(45) Choi, B.; Moon, B.; Seo, H.; Jeong, J.; Lee, H.; Seo, W. *Mat. Des.* **2000**, *21*, 567.

(46) Papoian, G. A.; Hoffmann, R. *Angew. Chem., Int. Ed.* **2000**, *39*, 2408.

(47) Saenger, W. *Naturwissenschaften* **1984**, *71*, 31.

+ $8\text{Au}_2\text{P}_3 \rightarrow 8\text{P}$ (black phosphorus) + $8\text{Au}_3\text{P}_2$) a hypothetical reaction relating Au_3P_2 and Au_2P_3 is 7.47 eV.

Conclusion

In this work, the electronic structure and chemical bonding of three ternary gold polyphosphides were analyzed. The DOS predicts that Au_2PbP_2 and Au_2TlP_2 should be metallic, Au_2HgP_2 a semiconductor. The metal element lines play an important role in determining metallic behavior in these unusual compounds. The Pb, Tl, and Hg chains do not undergo a pairing (Peierls) distortion, for good reasons. The small barrier for Pb motion along the chain axis and the still smaller barrier for Tl and Hg may also explain the large thermal parameters observed in the crystal structures along the chain axis and the refinement that required alternative sites for Hg (and Tl).

Liquidlike behavior of the metal chains is expected for any M in Au_2MP_2 . To guide future work, some hypothetical compounds (containing other atoms inserted into the Au_2P_2 channel) were also studied. The likely distances between atoms in these chains ranged from 3.05 Å (Au_2AuP_2) to 3.25 Å (Au_2IP_2). The results suggest that one could synthesize other ternary compounds based on the Au_2P_2 framework.

Acknowledgment. Calculations were performed in part at the Cornell NanoScale Facility, a member of the National Nanotech-

nology Infrastructure Network, which is supported by the National Science Foundation. Our work at Cornell was supported by the National Science Foundation through Grant No. CHE-0613306. This research was also supported in part by the National Science Foundation through TeraGrid resources provided by [NCSA].

Supporting Information Available: Details of all the COOP curves, OP and HP values of the three ternaries; the band structures, COOP curves, and TDOS of the Tl and Hg isolated chains; the TDOS, PDOS, COOP curves with OP and HP values of the Au_2P_2 lattice; a frozen band approximation of the Tl and Hg chains using isoelectronic Pb; further analysis of the Tl and Hg lines with corresponding structure geometries and band structures; the different one- and three-dimensional Pb structures predicted with DFT and corresponding energies of formation; the computed parameters (and corresponding figures) compared to the experimental parameters of the different ternary compounds predicted; the computed parameters obtained when threading other elements through the Au_2P_2 lattice, and their corresponding OP and HP values. This material is available free of charge via the Internet at <http://pubs.acs.org>.

JA806884A